Section A: Pharmacology, Toxicology, and Biochemistry.

Research Article

In silico analysis revealed the prognostic potential of a miRNA panel in lung carcinoma

Marwa Mohanad[1*], Rasha R. Fakhr Eldeen[1], Hoda K. Shamloula[1]

[1]Department of Biochemistry, College of Pharmaceutical Sciences and Drug Manufacturing, Misr University for Science and Technology, Giza, Egypt.

*Correspondence: marwa.almarzouky@must.edu.eg

Abstract

Background. This research aims to identify potential prognostic biomarkers for squamous cell lung carcinoma (LUSC) by implementing bioinformatics tools to unveil the relationship between microRNAs (miRNAs) and LUSC, specifically by identifying the miRNAs and their critical target genes.

Methods. We employed the Cancer Genome Atlas (TCGA)-LUSC dataset to identify differentially expressed miRNAs (DEmiRs) and genes (DEGs) utilizing R software. Subsequently, a lasso Cox regression survival model was developed to predict key prognostic DEmiRs. Their target genes were predicted using miRDB repository. Venn diagram was employed to identify the consensus genes shared between these target genes and DEGs in the TCGA-LUSC dataset. ClusetrProfiler analyzed Gene Ontology (GO) and KEGG pathways to comprehend these genes' biological functions. The STRING database and Cytoscape applications constructed the consensus gene protein-protein interactions network.

Results. Lasso model predicted 6 prognostic DEmiRs (hsa-miR1270, hsa-miR-1291, hsa-19b-2, hsa-miR-2277, hsa-miR-4791, hsa-miR-485) for LUSC with 96.67% sensitivity and 68.54% specificity. Venn diagram retrieved 906 consensus genes shared between DEGs and these 6 prognostic DEmiRs. These genes were mainly related to protein-binding, neuroactive ligand receptor interaction, retinoid metabolism, carcinogenesis, cell cycle, and system development. Network analysis in Cytoscape STRING applications identified 19 crucial genes (*SDC4, VCAN, BCAN, XYLT2, GPC1, GPC5, EGFR, EDNRA, EDN1, EDNRB, ERBB4, GNA14, GNAQ, CACNA1C, KCNQ1, KCND2, KCNH5, KCNB2, KCNQ5*) linked to lung carcinogenesis.

Conclusion. We developed a prognostic model reliant on 6 miRNAs that accurately predicted LUSC survival. These findings provide novel insights into lung carcinogenesis' underlying molecular mechanisms and potential biomarkers for prognosis and treatment.

Introduction

Lung carcinoma (LC), a highly prevalent and lethal form of cancer, is composed of various histological subtypes, the most prominent of which accounts for 85% of lung cancer cases; non-small cell lung carcinoma (NSCLC) [1]. Among NSCLCs, squamous cell lung carcinoma (LUSC) is the 2nd most prevalent subtype [2, 3]; however, it has a dismal survival rate of 20.2% [4]. In contrast to specific subgroups of adenocarcinoma that have benefited from precision medicine as a result of identifiable mutations, LUSC faces obstacles in this regard due to the absence of actionable mutations that could propel the development of personalized treatment approaches and ultimately improve patient outcomes [5].

Till now, there is no established means of discerning which premalignant lesions will progress to invasive cancer. The development and validation of a reliable method is crucial to identify individuals at high risk and improve global lung cancer screening [6]. Without this advancement, the comprehensive success of global screening initiatives remains a significant challenge. Thus, the distinctive molecular signatures and clinical behaviors of LUSC necessitate identification of comprehensive prognostic markers for precise patient management.

MicroRNAs (miRNAs) expression has been observed to be closely linked with numerous human diseases, notably cancer [7, 8]. MiRNAs are short, single-stranded RNA molecules that play a crucial role in controlling cellular processes such as development, proliferation, and neoplastic transformation [9, 10]. Their potential as biomarkers and drug targets is highlighted by their correlation with the progression of the disease [11-13]. A growing body of evidence indicates that miRNA-based therapies, which involve the regulation of miRNA expression, may hold great potential [14, 15]. Malfunctioning miRNAs play dual roles as either tumor suppressors or oncogenes, governing cell cycle progression, angiogenesis, invasion, proliferation, and apoptosis by modulating target genes negatively. Additionally, owing to its enhanced stability and broad range of applications, miRNA stands out as a promising biomarker for detecting LC [16].

The transcriptional control of miRNA is significantly influenced by genetic and epigenetic mechanisms, including DNA methylation and histone modification, which intricately regulate miRNA expression [17]. The progression of lung cancer has been suggested to be initiated by dysregulation of particular miRNA genes, which target messenger RNAs (mRNAs) [18]. The analysis of miRNA expression levels in serum and plasma exhibits considerable potential for prognostic and diagnostic purposes in the context of lung cancer [19]. By utilizing bioinformatics analyses, the intricate function of microRNAs in cellular proliferation and signal transduction can be better understood. Through a meticulous examination of discrepancies in miRNA expression between LC and healthy lung tissues, linked genes surface as prospective biomarkers that may aid in the diagnosis and prognosis of LC [20].

The acquisition of knowledge regarding the intricate molecular mechanisms and critical genes that are linked to LUSC is crucial in order to progress improvements of preventive and therapeutic strategies for this disease. Differential expression screening was employed in this investigation to ascertain the presence of differentially expressed genes (DEGs) and miRNAs (DEmiRs). DEG and DEmiR data were obtained from TCGA-LUSC dataset. Our aim was to employ a lasso Cox regression predictive model to identify potential prognostic miRNAs in LUSC. Following that, an exhaustive functional enrichment analysis was conducted on the genes that were shared among the DEGs and the predicted targets of the DEmiRs. The objective of this methodology was to elucidate the possible biological mechanisms that underlie these genetic associations in LUSC.

Materials and Methods

Retrieving tumor data set and differential miRNA and gene expression analysis

We acquired miRNA expression, gene expression, and relevant clinical data from 478 squamous cell lung carcinoma samples and 45 normal tissue samples sourced from the Cancer Genome Alas (TCGA) squamous cell lung carcinoma (LUSC) harmonized cancer datasets portal using TCGA assembler 2 [21]. Our analysis involved the use of the edgeR and limma packages within R Studio (version 4.2) to identify differentially expressed miRNAs (DEmiRs) and differentially expressed genes (DEGs). The criteria for determining differential expression were based on a threshold of a log_2-fold change exceeding 1.5 or less than -1.5, along with a false discovery rate (FDR) greater than 0.01.

Prognostic model based on DEmiRs.

Univariate Cox regression hazard proportional analysis was performed to determine the prognostic potential of individual DemiRs using survival and survminer packages of R and DEmiRs significantly associated with survival was at a significance of less than 0.05. Multivariate Cox proportional hazards regression analysis was performed to identify independent prognostic DEmiR significantly detected in univariate analysis. These prognostic DEmiRs were used as features to develop a lasso cox regression model using for the best prediction of survival outcome of patients with LUSC and stratify patients into high risk and low risk group. First, 75% of the dataset was allocated as the training set, while the remaining 25% was designated as the test set. Additionally, to prevent overfitting, the performance of the model was evaluated on separate validation sets, a 10-fold cross-validation technique was implemented on the training set. Metrics such as accuracy and the area under the curve (AUC) of the Receiver Operating Characteristic (ROC) curve were utilized to assess the performance of the model [22]. Kaplan Meier survival and log rank test was used to compare survival rates of high risk versus low-risk group.

Prediction of target genes of the DEmiR.

We employed the online repository miRDB (http://mirdb.org/) [23] to precisely predict the target genes associated with the prognostic DEmiRs. The identification of overlapping target genes shared among

the prognostic DEmiRs was achieved by utilizing the VennDiagram package within R software. We further enhanced our analysis by identifying consensus genes through a comparison between the predicted target genes and DEGs using the VennDiagram package in R.

Enrichment analysis of the consensus genes

Pathway enrichment analysis for Gene ontology (GO) and KEGG pathway was carried out using cluster Profiler package within R. The significance level was set $p<0.05$.

Building and examining consensus gene-driven PPIs Networks

The Search Tool for the Retrieval of Interacting Genes/Proteins (STRING) was utilized to construct a network of significant protein-protein interactions (PPIs) of the consensus genes with high confidence level of ≥ 0.7 as previously described [24]. Subsequently, the obtained results were visualized using Cytoscape String APP (Cytoscape, version3.7.1) [25]. For network analysis, the CentiScaPe plugin within Cytoscape was employed to measure the centrality parameters such as node degree, proximity centrality, and other critical metrics in the PPIs network. This allows the identification of critical nodes and understanding their importance within the network context [26]. Furthermore, biological functional modules within the intricate interaction networks of consensus genes were identified utilizing the Molecular Complex Detection (MCODE) plugin within Cytoscape. To precisely extract relevant clusters based on their internal connectivity and biological importance within the networks, the MCODE plugin was customized with specified parameters (degree cutoff ≥ 10, node score cutoff ≥ 0.2, kappa-score (k-core) ≥ 2, and max depth 100) [27].

Results

Differential expression of miRNAs in squamous lung carcinoma

Bioinformatic analysis of the TCGA-LUSC revealed 67 downregulated miRNAs and 405 upregulated miRNAs with statistical significance (*Padj>0.01*) as illustrated by volcano plot (Fig.1a). There were 5,991 DEGs in total; 2,210 were downregulated and 3,781 were upregulated (Fig.1b).

Univariate and multivariate survival analysis according to DEmiRs

Using univariate Cox regression, 14 DEmiRs were identified to be significantly associated with unfavorable outcomes in LUSC patients ($p<0.05$). These DEmiRs include hsa-miR-1306, hsa-miR-106a, hsa-miR-106b, hsa-miR-1270, hsa-miR-1291, hsa-miR-19b-2, hsa-miR-2277, hsa-miR-3170, hsa-miR-3200, hsa-miR-376a-2, hsa-miR-4791, hsa-miR-485, hsa-miR-6808, and hsa-miR-744 (Table 1). Prognosis in LUSC patients was independently predicted by hsa-miR-1270, hsa-miR-1291, hsa-miR-19b-2, hsa-miR-2277, hsa-miR-4791, and hsa-miR-485, according to multivariate Cox regression analysis as shown in Table 2 ($p<0.05$).

The differential expression patterns of the 6 independently prognostic miRNAs were observed in LUSC. hsa-miR-1270, hsa-miR-19b-2, and hsa-miR-2277 exhibited upregulation, whereas hsa-miR-1291, hsa-miR-4791, and hsa-miR-485 demonstrated downregulation (Fig.1a).

Predictive model for prognostic outcomes in squamous cell lung carcinoma patients.

Lasso cox survival model based on the 6 miRNAs identified in Cox regression analysis predicted survival outcome on the test set with an accuracy of 76%. The distribution of LUSC's patients' status according to risk score is illustrated in Fig.2a. A ROC curve was constructed according to the true death events on the test set compared to the model's predicted probabilities, showed an AUC of 0.89 with model's sensitivity and specificity of 96.67% and 68.57%, respectively (Fig.2b). According to Cox hazard risk computed based on the coefficients of each predictor, the patients were categorized into high-risk group and low risk group. The log rank test and Kaplan-Meier curve survival analysis revealed a statistically significant difference in survival rates of the high-risk (31.38%) versus low-risk (83.19%) groups ($p<0.001$) (Fig.2c).

Prediction of target genes for the independently prognostic miRNAs

We utilized the miRDB database (https://mirdb.org/) to conduct a predictive analysis of target genes linked to the 6 distinct independent prognostic miRNAs. A Venn diagram was employed to visualize the overlap among these prognostic miRNAs and their shared target genes. Upon juxtaposing the target genes associated with the 6 independent prognostic miRNAs with the pool of 5991 DEGs identified in LUSC patients, we identified 906 consensus genes (Fig.3a). Specifically, these consensus genes—comprising 151, 237, 240, 44, 109, and 227 genes—were linked respectively to hsa-miR-1270, hsa-miR-1291, hsa-miR-19b-2, hsa-miR-2277, hsa-miR-4791, and hsa-miR-485, considering the shared target genes among these prognostic miRNAs (Table 3 and Fig.3b)

Enrichment analysis of consensus genes

The Gene Ontology enrichment analysis, conducted via clusterProfiler, identified 48 significantly enriched GO terms associated with the set of 906 consensus genes. These terms encompassed diverse biological and metabolic functions, including but not limited to system development, carboxylic acid transport, regulation of post synaptic membrane potential, protein binding, membrane-associated activities, neurons, and nervous system development (Fig.4a). The GO term "protein binding function" demonstrated a strikingly significant statistical association, showcasing a remarkably low p-value of 1.475e-11. This term was notably linked to the largest cluster of consensus genes, totaling 723, emphasizing its pivotal role within this gene set. Furthermore, within its GO context, this term was found to be associated with growth factor binding ($p = 1.55e-04$) and transmembrane transport binding ($p = 2.998e-03$), indicating potential connections to crucial cellular processes related to growth
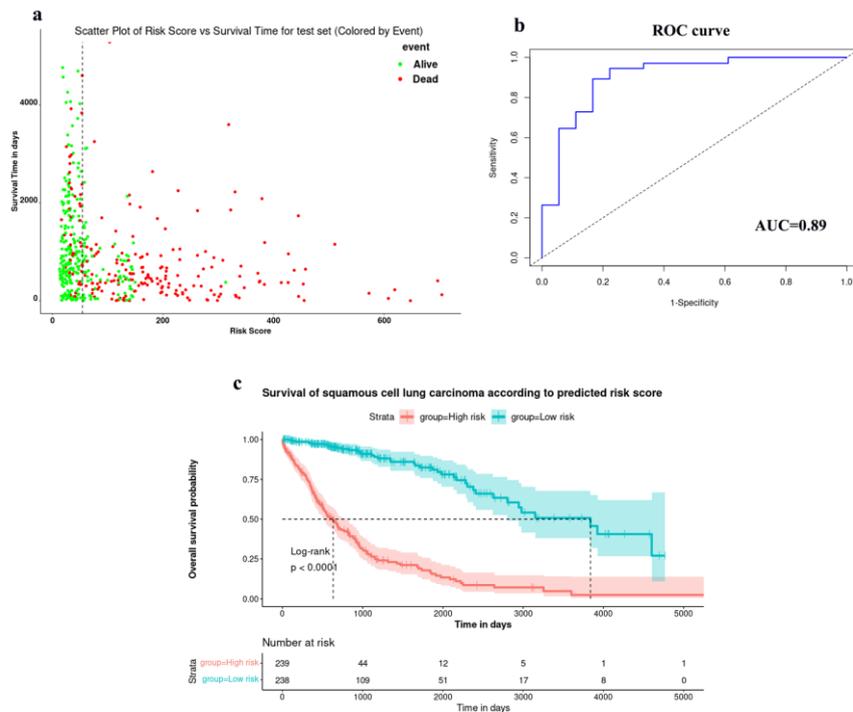
Table 1. Univariate Cox proportional hazard regression of the miRNAs associated with survival outcome in patients with squamous cell carcinoma.

miRNA	HR	95% CI	*p*-value
hsa-miR-1306	1.001	1.000-1.001	0.0017**
hsa-miR-106a	1.002	1.000-1.003	0.038*
hsa-miR-106b	1.002	1.001-1.004	0.043*
hsa-miR-1270	1.003	1.000-1.004	<0.001**
hsa-miR-1291	0.42	0.23-0.61	<0.001**
hsa-miR-19b-2	1.004	1.17-11.6	<0.001**
hsa-miR-2277	1.003	1.40-74.1	<0.001**
hsa-miR-3170	1.005	1.002-1.006	<0.001**
hsa-miR-3200	1.002	1.000-1.004	0.014*
hsa-miR-376a-2	1.004	1.003-1.005	<0.001**
hsa-miR-4791	0.62	0.48-0.81	<0.001**
hsa-miR-485	0.57	0.41-0.79	<0.001**
hsa-miR-6808	1.001	1.000-1.005	<0.001**
hsa-miR-744	1.002	1.001-1.003	0.027*

hsa: homo sapiens, HR: hazard ratio, CI: confidence interval

factor interactions and transmembrane transport activities. This highlights the importance of protein binding function in various biological mechanisms, underscoring its potential significance in these particular pathways within the context of the identified consensus genes. The KEGG pathway enrichment analysis of the consensus genes revealed 32 pathways significantly enriched including, neuroactive ligand receptor interaction, retinol metabolism, cell cycle, DNA replication, chemical carcinogenesis, nicotine addiction and cancer pathway. Noticeably, neuroactive ligand receptor interaction

pathway showed the largest cluster of consensus genes (n=72) of *p*-value=4.2e-8 (Fig.4b).

Building and examining consensus gene-driven PPIs Networks

The 906 consensus genes were examined within the STRING database to establish PPIs network, where a stringent confidence score of 0.7 was applied. The resulting network was visualized using Cytoscape, represented as an undirected graph. In this graphical representation, genes were denoted as individual nodes,

Fig.1. Volcano plot of differentially expression showing (a) DEmiRs and (b) DEGs in LUSC. Red dots signify upregulation with LogFC >1.5 and blue dots signify downregulation. No change is presented by grey dots.

Fig.2. Lasso prognostic model prediction of survival risk score based on the 6 prognostic DEmiRs in LUSC. (a) The distribution of patient's survival according to risk score. (b) ROC curve for assessing the performance of lasso prognostic model in LUSC. (c) Kaplan-Meier survival analysis in high-risk versus low-risk groups.

and the edges between these nodes represented interactions among the encoded proteins [28]. This initial network comprised 141 nodes and 310 edges (Fig. 5a). Employing the CentiScape application, we identified 61 hub genes meeting the criterion of having a degree of ≥5. Subsequently, a refined network composed of 61 nodes and 141 interactions was delineated (Fig. 5b).

Table 2. Multivariate Cox proportional hazard regression of the miRNAs associated with survival outcome in patients with squamous cell carcinoma.

Factor	HR	95% CI	p-val
hsa-miR-1306	1.001	0.81-1.002	ns
hsa-miR-106a	1.003	0.78-1.005	ns
hsa-miR-106b	1.002	0.85-1.003	ns
hsa-miR-1270	1.003	1.001-1.005	<0.001**
hsa-miR-1291	0.53	0.35-0.72	<0.001**
hsa-miR-19b-2	1.000	1.000-1.001	<0.001**
hsa-miR-2277	1.003	1.001-1.005	0.002*
hsa-miR-3170	1.005	0.91-1.006	ns
hsa-miR-3200	1.002	0.78-1.004	ns
hsa-miR-376a-2	1.003	0.82-1.005	ns
hsa-miR-4791	0.62	0.58-0.76	0.009*
hsa-miR-485	0.48	0.35-0.70	<0.001**
hsa-miR-6808	1.003	0.36-1.004	ns
hsa-miR-744	1.001	0.58-1.003	ns

hsa: homo sapiens, HR: hazard ratio, CI: confidence interval, ns: non-significant
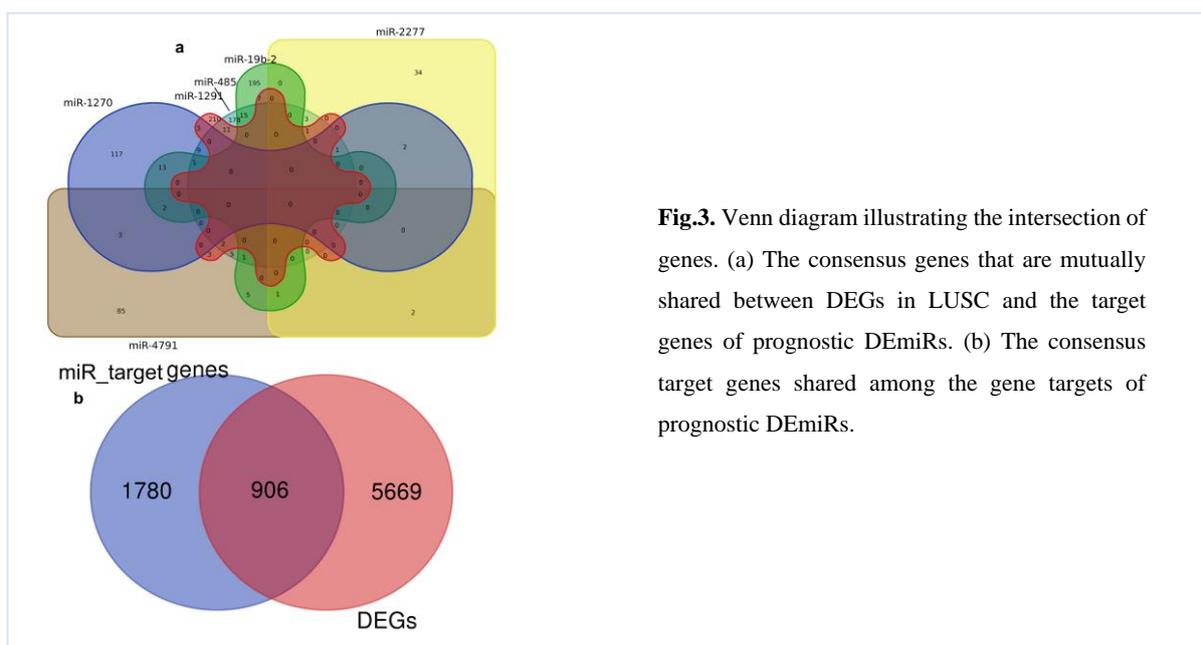
Fig.3. Venn diagram illustrating the intersection of genes. (a) The consensus genes that are mutually shared between DEGs in LUSC and the target genes of prognostic DEmiRs. (b) The consensus target genes shared among the gene targets of prognostic DEmiRs.

Further analysis using the MCODE plugin unveiled three distinct clustering modules within the hub genes. These modules comprised 19 critical genes, including, syndecan (*SDC4*), verican (*VCAN*), brevican *(BCAN)*, xylosyltransferase2 *(XYLT2)*, glypican1 *(GPC1)*, and glypican5 (*GPC5*) in module 1 (score=7.714); epidermal growth factor receptor (*EGFR*), endothelin receptor type A *(EDNRA)*, endothelin 1 *(EDN1)*, endothelin receptor type B *(EDNRB)*, erb-b2 receptor tyrosine kinase 4 *(ERBB4)*, G protein subunit alpha 14 *(GNA14)*, and G protein subunit alpha q *(GNAQ)* in module 2 (score=4.8); and calcium voltage-gated channel subunit alpha1 C (*CACNA1C)*, potassium voltage-gated channel subfamily Q member 1 *(KCNQ1)*, potassium voltage-gated channel subfamily D member 2 (*KCND2*), potassium voltage-gated channel subfamily H member 5 (*KCNH5*), potassium voltage-gated channel subfamily B member 2 *(KCNB2)*, and potassium voltage-gated channel subfamily Q member 5 (*KCNQ5)* in module 3 (score=4.8) (Fig.5c, d, e).

Regarding their target development level, *SDC4, SDC5, VCAN, BCAN, XYLT2, GPC1, GPC5, GNA14, EDN1, GNAQ,* and *KCNB2* were classified as Tbio, indicating that their corresponding proteins possess experimental Gene Ontology terms. Meanwhile, *EDNRA, EGFR, EDNRB, CACNA1C, KCNQ1, KCND2, KCNH5, ERBB* and *KCNQ5* were categorized as Tclin, designating their corresponding proteins as targets for approved drugs.

Discussion

Recently, miRNAs provoked scientists' investigations due to their participation in tumor incidence and progression [29]. The availability of miRNA data across various cancer types enables comprehensive miRNA profiling. Understanding the mechanisms underpinning tumorigenesis holds promise for advancing cancer therapy by facilitating targeted interventions.

Within the scope of this investigation, we have successfully identified DEmiRs and DEGs associated with LUSC utilizing datasets sourced from the TCGA. Then,

we developed a lasso prognostic model based on the 6 independent prognostic miRNAs (hsa-miR-1270, hsa-miR-1291, hsa-miR-19b-2, hsa-miR227, hsa-miR-4791, and hsa-miR-485) identified in multivariate Cox regression survival analysis. These miRNAs were selected as potential prognostic markers due to their relevance in the context of the research objective. Integrating these 6 miRNAs into the prognostic model, it is anticipated that a more accurate prediction of the prognosis can be achieved with a sensitivity of 96.67% and specificity of 68.57%. A comprehensive analysis was conducted to identify consensus genes by intersecting the DEGs with the target genes predicted for the prognostic miRNAs utilizing the miRDB repository. A total of 906 consensus genes were successfully obtained through this analysis. Further enrichment analyses of GO and KEGG pathways demonstrated that the identified consensus genes primarily participate in signaling pathway of neuroactive ligand receptor interaction, retinol metabolism, cell cycle, DNA replication, chemical carcinogenesis, nicotine addiction, protein binding, system development, carboxylic acid transport, regulation of post synaptic membrane potential, membrane-associated activities, neurons, and nervous system development. By employing STRING Cytoscape applications, we analyzed the PPIs that occurred among the 906 consensus genes. The implementation of Cytoscape's extensions, CentiScape and MCODE, revealed 19 crucial genes, *SDC4, VCAN, BCAN, XYLT2, GPC1, GPC5, EGFR, EDNRA, EDN1, EDNRB, ERBB4, GNA14, GNAQ, CACNA1C, KCNQ1, KCND2, KCNH5, KCNB2,* and *KCNQ5* implicated in the pathogenesis of LUSC.

Notably, hsa-miR-1270, hsa-miR-19b-2, and hsa-2277 were found to be upregulated in LUSC, whereas hsa-miR-1291, hsa-miR-4791, and hsa-miR-485 were found to be downregulated. Additionally, our analysis unveiled the following differential expression patterns of critical genes involved in the pathogenesis of LUSCs: In contrast to the upregulation of *VCAN, BCAN, XYLT2, GPC1, EGFR, EDN1, KCND2, KCNH5, KCNB2, ERBB4, EDNRA, GNA14, SDC4* and *KCNQ5*, the downregulation was
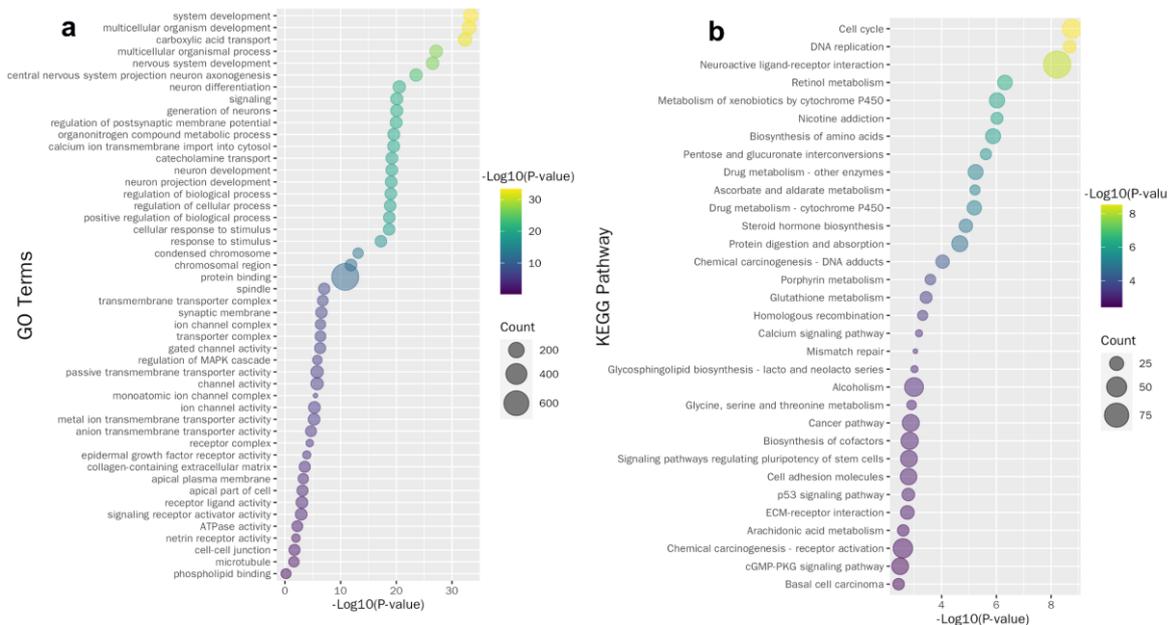
Fig.4. Enrichment analysis on a pool of 906 consensus genes. (b) Enrichment analysis for GO. (b) and KEGG pathways. The graphical representation utilized -log10 P-values on the x-axis and represented various GO terms and KEGG pathways on the y-axis. The size of the bubbles corresponded to the count of consensus genes, visually emphasizing their prevalence in the analyses.

observed in *GPC5, EDNRB, GNAQ, CACNA1C,* and *KCNQ1*.

Notably, *SDC4*, and *GPC5* were targeted by hsa-miR-1270, while hsa-miR-1291 targeted *KCNQ5, XYLT2, KCNQ1,* and *BCAN*. Additionally, hsa-miR-485 was linked to the targeting of *KCNQ5, EDNRA, GNA14, GPC1,* and *VCAN*. Moreover, the genes *EDNRB, EDN1, GNAQ, KCND2, KCNH5, CACNA1C, EGFR,* and *KCNB2* were targeted by hsa-miR19b-2. Lastly, *ERBB4* was identified as the target for hsa-miR-2277 and *KCNQ5* and was identified as the target for hsa-miR-4791. These

associations underscore the intricate regulatory relationships between the prognostic DEmiRs and critical genes, providing insights into potential mechanisms influencing their expression and function within the context of our investigation.

Notably, hsa-miR-1270 specifically targeted *SDC4* and *GPC5*, whereas hsa-miR-1291 targeted *KCNQ5, XYLT2, KCNQ1,* and *BCAN*. Moreover, hsa-miR-485 regulated *VCAN, KCNQ5, EDNRA, GNA14*, and *GPC1* expression. Furthermore, hsa-miR19b-2 targeted the following genes:
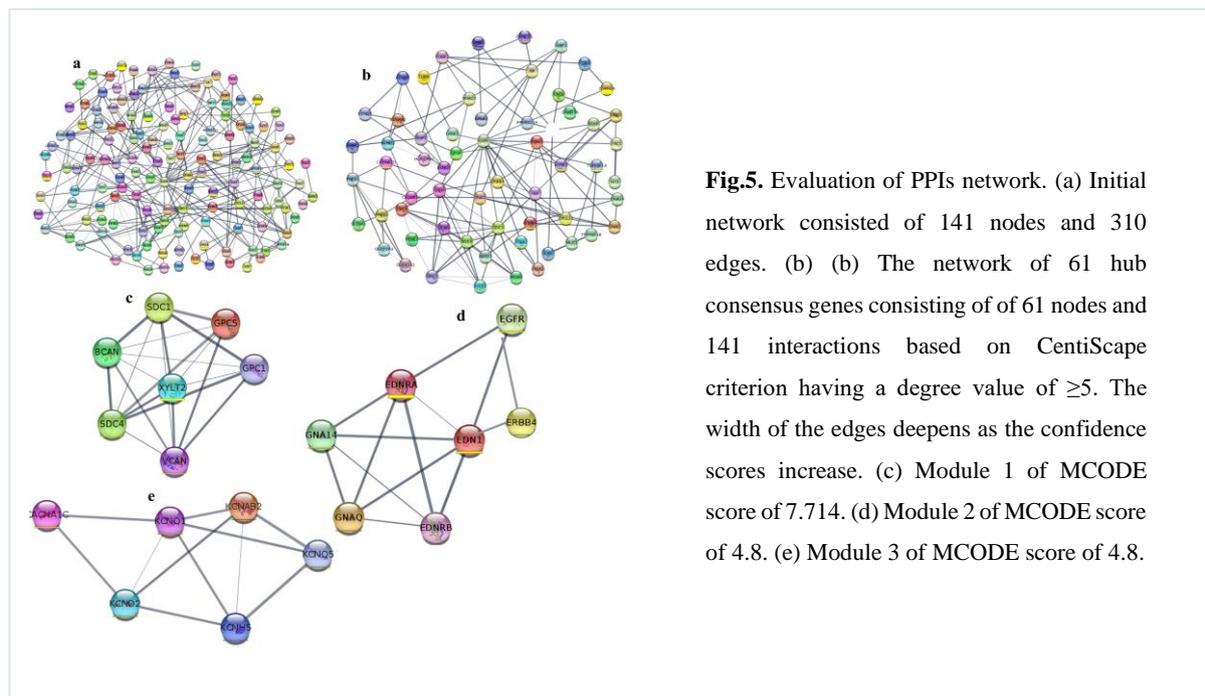

Fig.5. Evaluation of PPIs network. (a) Initial network consisted of 141 nodes and 310 edges. (b) (b) The network of 61 hub consensus genes consisting of of 61 nodes and 141 interactions based on CentiScape criterion having a degree value of ≥5. The width of the edges deepens as the confidence scores increase. (c) Module 1 of MCODE score of 7.714. (d) Module 2 of MCODE score of 4.8. (e) Module 3 of MCODE score of 4.8.

Table 3. The consensus genes common among the target genes of the 6 prognostic miRNAs and the DEGs of patients with squamous cell lung carcinoma.

miRNA	Consensus genes
hsa-miR-1270	*N4BP2L1, UBASH3B, OLA1, ZIC5, EPPIN, LAMB4, ANKRD44, SENP5, AFP, GLI2, STOML3, CD276, UNC5D, TCF20, SLC24A2, SH3BGRL2, DNAAF3, ENTPD3, XKR9, LYSMD1, HLA-DQA1, UNC45B, HAS1, SPTBN1, RFC5, BORCS7, **SDC4,** PDE1C, MAN1A1, ZDHHC15, TUBB, RBM46, BCL11B, LIN9, TPD52L1, UNC5CL, TET3, ATP12A, KCNA4, CNDP1, HEG1, DENND2C, DBX2, MEF2C, CACNA1E, STON2, ANTXR2, TRIP6, GLRA3, BMP2, CEACAM1, CASP14, GALNT2, CNGB3, CNNM1, **DCX,** TRPM3, TMEM183A, A1CF, REPS2, ZNF286A, COL22A1, OTULINL, TJP1, CALN1, F8, PROM2, ANGPTL7, SORL1, FGL2, NOVA2, RBPMS, ZBTB20, CTSE, OLFM3, GRHL2, TAF2, CDKL5, DIXDC1, YWHAQ, NEGR1, OR7D2, ADCY2, LHX2, FAM189A1, **GPC5,** KRT37, CELSR2, PRR29, HMGA2AS1, CADM4, DLX3, FCGR1B, AQP11, LRRC74B, SNX20, FLRT3, LGI1, SLC39A8, FCGR1A, PAK6, KCNB1, NFATC2, HLA-DQA2, MAP3K19, OLFM4, MTFR1, CHRNB2, ILF2, ST8SIA6, SHISA9, ANXA3, DDX10, UBL3, TXNDC17, ZNF385D, NOL10, SHISA3, PDZD2, HPSE2, ABCA3, ANAPC7, TMEM236, PLCL2, CADPS2, HMGCLL1, SPN, ULBP3, SH2D4B, LYSMD3, AMER1, AHCYL2, EMCN, SLC1A1, GPR26, WWC1, BMP8B, SHISA6, LMCD1, CPNE6, MYOCD, CGN, HS6ST3, USP31, FABP5, RAG1, DOK3, EPHA6, IL17RD, HECW2, STX12*
hsa-miR-1291	*REEP2, PGM5, CYP2C18, VASH1, ST6GALNAC6, XKR7, VWA5A, RBFOX1, MAGEA11, KIAA1549, MUC22, TGM4, IMPA2, LMOD1, SLC6A3, ERMP1, WNT11, UNC13B, SNRPB, DYNC1I1, CABP7, PLA2G4C, MAN1C1, FBXO41, SH2D5, KREMEN1, **KCNQ5,** IQSEC3, GPM6A, ARL4C, NPTXR, SRSF9, VSIG4, EPHB2, LIMS2, CDT1, PHYHIP, HMOX1, FAM189A1, C11orf21, FGFR3, AQP1, CD74, CEMIP2, MYBL2, DNMT3A, NPTX2, CENPO, FAXDC2, PKP1, RFWD3, PACSIN1, DRC3, PRIMA1, TCF19, IL6R, CACNA1I, DBN1, MMP24, ARHGDIB, KIAA1522, LMO4, FGD1, RNF125, SLC6A11, SH3GL1, MRPS26, FGF11, SYT2, HAP1, DIRAS1, GLRX, SLC5A6, ARHGEF4, HIC1, MYO19, HOXC6, DOK4, RAX, CDKN2A, LRRC10B, CHRNA7, RAB3B, ALDOC, VNN2, C16orf89, GALNT16, LGR4, RAB38, CXCL12, MSX2, BTBD11, WIPF3, RNF128, WSCD2, OGDHL, LRRK2, WDR5,TTYH3, SAPCD2, PLCE1, NAT8L, UBTD1, RS1, SLC6A17, MUC1, ATG4D, FAAP24, TRMT2A, EN2, SLC7A5, BMPR2,CD1E, ADGRG1, **XYLT2,** MPP2, GALNT6, SDC1, XRCC3, MEF2C, RASSF2, ADAM11, NYAP1, EDARADD, CCDC137, CYSRT1, SBK1, EIF4EBP1, LPO, CCDC40, ADGRB1, TWNK, CALML5, KCNN3, SDK2, **KCNAB2,** MAGEA8, HES5, SCN2B, ZNF423, SNRK, C10orf105, DOK7, TMEM184A, CELF5, MTHFR, FCRL5, MICALL1, TRIM58, **KCNQ1,** TAL1, RNF43, SAMD14, SLC6A20, SPRN, SIRT7, KRT76, CFLAR, MAP1B, LIN7A, WNK4, ABCC1, LGALS12, **BCAN,** CHAC1, MYLK2, CFAP73, EPHB3, SLC39A5, KCNK5, FOXE1, OVOL1, NTSR1, SLC2A1, CHST7, RASGEF1A, SPEG, CNTN2, KLHDC7A, LSM14B, ARHGAP31, SLC1A7, FAM131A, PRKAG3, LIME1, SYT6, TMCC2, NKPD1, DERL3, CPLX2, LPIN3, ADAMTS14, GRM4, CCDC9B, PNMA3, ANPEP, FAM83H, LRRC32, UNC45B, ALDH1L2, LAD1, LEFTY2, TAS1R3, REEP6, GBP4, RUNX1T1, CABLES1, YKT6, GAREM2, CNR1, FLT3, TTLL10, USH1C, PIWIL3, TNFRSF1B, KRT80, GNMT, FERMT2, IGF1R, SEMA3F, TMEM105, RIN3, LRRC75A, SGIP1, SYNPO, ALPK3, HPCAL4, EMX1, TGM5, CDK4, EPO, TNS1, KNDC1, MOBP, TSKU, HPN, RALGAPA2*
hsa-miR-19b-2	***EDNRB,** LIN28B, CFL2, FYTTD1, GATM, ZNF578, NRXN1, PLEKHO2, NTS, SLC6A8, PGR, SGIP1, SLC39A8, ACACB, SLITRK4, TRIM7, RBMS3, **EDN1,** GRIK2, CP, BCL11B, NEK7, GSTA2, CREBRF, FLRT3, TRPS1, ELOVL6, FKBP5, PRDM13, RUNX2, TNS4, FAXC, CENPN, PHYHIPL, SEZ6L, NR4A3, ACVR1L, FHL5, MSRB3, PDE1C, ALDH1A2, HSPB8, UNC5C, CCN2, POLQ, CREB3L1, NR2E1, ANKS1B, GABRB2, MS4A4A, PPARGC1A, **GNAQ,** CENPF, ESCO2, ELAVL4, PLXDC2, MEX3D, DYDC2, KIAA1549, **KCND2,** NTN4, ARRDC3, RALGPS2, ZBTB20, ZNF483, STEAP4, TMPO, NEGR1, ALDOC, ARHGAP36, PHACTR1, MSI2, USP28, CBLN2, PHF6, FAM189A2, ONECUT2, PLCXD3, CCDC141, MYRIP, CAND1, **KCNH5,** FGD4, OLIG3, SNX20, EGR2, AGMAT, MAN1A1, CHEK1, FBXO32, SYT9, GATA4, MFSD4A, COL24A1, TET1, NECAB1, HOXA13, TRIM2, ADAM23, FCGR2A, ARHGAP11A, SESN3, PRDM6, P2RX7, MICAL2, LCLAT1, RAB3B, CBARP, EHHADH, ALOX12B, LRRC2, XPO1, NCMAP, GUCY1A1, PRTG, PTPRB, SCARF1, RHBDL2, **CACNA1C,** ACSL1, KDM5B, ABCC1, STC2, ADGRL2, RBPMS, ACAP2, CNTN1, ELOVL2, FAM111B, **EGFR,** CADM2, TFAP2A, ADCY10, DOK3, SDK1, C7, SLC16A6, SFRP1, SLC14A1, JPH3, SLC43A3, TIMP3, SERTM1, KRT36, PRRG1, MZT1, MEOX2, FOXF1, GPR63, SASS6, SGCZ, KIAA1549L, P2RY12, BCL11A, RASGRP3, ZNF138, MARVELD3, PCDH19, ITGA1, SLC7A14, LRRC74B, **KCNB2,** TMTC3, IGF2BP1, RASSF10, MICAL3, TSPYL5, NAV1, GYPE, NTN1, MYH11, IGFBP5, DNMT3A, TMPRSS11E, PSAT1, TBL1XR1, USP31, MCMDC2, PRKCI, NTRK2, STXBP5L, ZNF716, TLCD2, DAZL, UNC80, NCAPG2, PYCR3, TGFB2, DPPA2, KCNB1, CNTNAP2, C1orf74, ANTXR2, MAPK6, XYLB, CCNF, PSMC3IP, STAC, FGF12, PRKG1, DCUN1D1, TRMT61B, KIF24, CPEB4, CHRNA9, CERS6, HEG1, KIF26B, BDNF, NSG2, SECISBP2L, MAGI1, LINGO2, ZEB1, GNG2, HEBP2, CYCS, TAL1, TLX2, ST6GALNAC3, IL6ST, C5AR1, SHISA9,*

	FNIP2, SYNM, FCRL4, OTX1, EMX2, MED12L, PABPC5, PDAP1, FAM155A, CYTIP, AQP4, TLL1, SOX21, PMS2, SERINC1, CACNA1B, SCIMP
hsa-miR-2277	*NRSN1, CGNL1, IGLON5, NTNG1, CCR2, TUBB3, GRIA2, BCL11A, C6orf141, NAA40, TSPAN5, VEGFD, TRIM9, SLC12A8, VIPR1, NT5DC3, TAPT1, NKX2-1, LRRC52, HGF, MTCL1, RAPGEF5, STX12, RCC2, NLGN1, HSPD1, SHISA7, TSPEAR, PEAK1, SLC8A2, WASF3, CHST2, MAP3K13,* **ERBB4,** *U2SURP, HOXC13, TET3, ZIC5, MCF2, PGLYRP4, RAB38, TTC28, ADA2, CDK15*
hsa-miR-4791	*SLITRK1, ADGRE3, CACNA1D, CTCFL, CADM1, S1PR1, PCDH9, PGM2L1, DVL3, CHRM5, ETV1, LGI1, EFEMP1, VTCN1, ERP27, DHFR, ERLIN2, ZIC3, CYP24A1, SGCD, UTP25, ITGA2, PTCHD4, IL11, TRIM10, TRIM22, CDH8, ZBTB20, CENPH, MAN1A1, MYH11, FNDC1, GDF10, ELAVL2, GUCY1A1, KANK2, GAN, FGL1, KLRF1, IFT140, XPNPEP3, RUNX1T1, HTR3E, MAP3K13, SLC38A1, STMN1, ENO4, GMNC, HMGA2, DIAPH3, PASD1, LAMP3, PSD3, CASP2, ABCA8, AOC3, GUCY1A2, RASSF6, PRKG2, SCN1A, LRPPRC, BTBD11, NCOA7, AR, WASF3, SEMA4B, CCDC73, DCUN1D5,* **KCNQ5,** *SEMA5B, SLC25A21, HOXD13, USH2A, CLDN2, NCAM2, HLA-DQA2, RAB8B, PDE2A, HABP2, KCTD16, TBL1X, CPEB3, BCL11A, TRIM2, HNF1B, EIF4E3, SMPD3, SCN9A, GSTM3, GRIN2A, CAND1, RBFOX1, ZNF608, ONECUT2, ITGB8, FOXP3, PTGFRN, GPR37, IL1RAP, UBL3, CIP2A, CD1E, HLA-DPB1, LRRN4CL, EGR2, CDKL2, PRIM2, LOXHD1, KCTD1*
hsa-miR-485	*CREBRF, ELAVL2, PDZD2, CNR1, ADCYAP1, SMPX, PPARGC1A, RUNX2, GOLGA8A, NWD2, RCN2, RYR2, MEI4, GALC, SLC7A14, P4HA3, FBN2, LEPR, CACNA1B, FCHO2, NRXN1, JAG1, ARHGAP20, GLRX3, CDH19, MUC15, RNF145, PLCL2, CPED1, SLC40A1, ST6GAL2, KIF21A, UGT8, ULBP1, NFIX, GDA, RAI2, SNAI2, DLC1, CCDC68, XG, KLF6, PCDH7, RAB38, CCDC85A,* **KCNQ5,** *PMP2, PCDHAC1, PEAK1, KBTBD8, PCDHAC2, PCDHA10, PCDHA3, KMT5A, PCDHA12, GTF3C3, MGARP, TCTEX1D1, ITM2A, CDK16, GRID1, TBX15, CKAP5, ALDH18A1, PDIA6, MZT1, UNC80, NAT8L,* **EDNRA,** *NUDCD1, CD36, CPOX, C6orf201, MATN3, FBXO45, TAC1, CCN1, BTG2, ABTB2, SLC6A15, MCM8, LIMD1, MCM6, ARHGAP6, RBM28, ZIC5, GNA14, DACH1, PM20D2, RCCD1, MFN1, C11orf87, HS6ST3, LMOD1, AQP9, KPNA2, HACD4, CADM2, GCNT4, SLC16A9, CEACAM1, ZMAT1, MSI2,* **GPC1,** *MELK, EHHADH, TMEM215, CLEC4M, STX2, SLC6A11, TRDN, TMEM108, OXGR1, PDE4D, CASK, GIMAP6, MYCT1, WIF1, CADM4, GPM6A, ATAD5, KCNB1, PPP1R14C, CALCRL, BMPR2, TTPAL, SCAI, TRIM2, EPHA7, GPD1L, FAM3C, CPLX2, CHRDL1, MYCN, EIF3B, ZNF367, ABCC2, PDE3B, KIF23, PAG1, LRRK2, HEPACAM2, RIPOR2, LHX1, TRABD2A, ARHGAP29, SLC6A20, PREX2, ABRACL, REEP1, RET, IL6ST, REPS2, PPM1K, MAGOHB, FCAR, DOK6, ZIC2, DCUN1D5, KLRD1, WDR17, HSPA6, SOX7, LRAT, KIAA0513, CCR2, NTRK3, RGL1, IL1RN, CORIN, SLC8A1, UNC5D, CDH8, CHGA, GOLGA7B, SMAD7,* **VCAN,** *CCDC150, BTBD11, MPP6, P2RY1, LDB2, ADAM23, CKAP2, RBM46, SDHAF3, ZNF273, TPD52L1, TRIM10, STMN2, MTCL1, SOX9, C17orf75, SECISBP2L, MCM10, SCN9A, SCML2, SMIM14, ZC3H12B, ABCG2, POLR3G, PAQR3, LIN7A, KCNK2, ATG9B, PTPRM, RGS5, MBIP, INPP5K, CERKL, FOXE1, CNTN5, WNK3, FCRL4, UBA6, PRDX1, STK26, PI15, SLC5A12, TMEM178B, XPR1, CCDC144NL, PRSS35, PTPRF, TNFSF15, CLEC12A, UMPS*

Genes in bold signifies critical consensus target genes visualized in PPIs networks.

EDNRB, EDN1, GNAQ, KCND2, KCNH5, CACNA1C, EGFR, and *KCNB2*. *ERBB4* was ultimately determined to be the target of hsa-miR-2277, while *KCNQ5* was found to be the target of hsa-miR-4791. These correlations highlight the complex regulatory connections that exist between the prognostic DEmiRs and crucial genes, thereby offering valuable insights into possible mechanisms influencing their expression and functionality in the context of our investigation.

The miR-1270 expression pattern is multifaceted in comparison to our findings that link upregulation of miR-1270 with an unfavorable prognosis in LUSC. In particular, an earlier investigation documented the inhibition of hsa-miR-1270, which was linked to the prevention of tumorigenesis in papillary thyroid carcinoma [30]. However, discerning the prognostic significance of hsa-miR-1270 across distinct cancer types has yielded contradictory and inconsistent findings. Recent investigations have spotlighted the suppressive role of hsa-miR-1270 in breast cancer [31] and glioblastoma cancer [32] progression and metastasis, aligning with its association with a more favorable prognosis for patients in these particular settings.

Conversely, the upregulation of hsa-miR-1270 has been linked to a poorer prognostic outcome in osteosarcoma [33] and gastric malignancies [34]. Notably, we demonstrated that that hsa-miR-1270 induced upregulation of *SDC4*, but downregulation of *GPC5*. Our findings align with prior research that has established the regulatory influence of miR-1270 on *GPC5* expression in the progression of NSCLC [35, 36], emphasizing its potential role as a substantial regulator within the context of our investigation into LC progression.

Corroborating our findings, another study found lower *GPC5* expression in LC tissues than adjacently noncancerous cells. The presence of GPC5 appears to suppress LC cell migration and invasion [37]. Additionally, it has been reported *GPC5* possesses the capability to induce G1/S phase arrest in these cells, improving prognosis [38].These disparate associations underscore the intricate and multifaceted nature of hsa-miR-1270's role in cancer progression and prognosis. While our findings support the concept that hsa-miR-1270 upregulation is associated with an adverse prognosis in LUSC, the divergent outcomes across different cancer types emphasize the necessity for a nuanced and context-

specific interpretation when assessing the prognostic significance of hsa-miR-1270 in distinct cancer landscapes.

SDC4, which is classified as a member of the syndecan family of cell surface proteoglycans and is encoded by the *SDC4* gene, functions as a receptor for a diverse array of extracellular matrix (ECM) components and growth factors. It plays a crucial function in coordinating the processes of cell-matrix adhesion, migration, and signaling pathways [39]. Considering the shared characteristics of tumor progression among various cancers, it has been demonstrated that *SDC4* influence the adhesion and metastasis of breast cancer cells, according to a study by Beauvais and Rapraeger (40). According to Mundhenke, Meyer (41), SDC4 is additionally involved in breast carcinoma through the formation of complexes with fibroblast growth factor 2 (FGF2) and its receptor FGFR-1. This interaction facilitates FGF signaling within breast carcinoma. Notably, previous research has revealed that the suppression of hsa-miR-1270 modulates *SDC4* expression, potentially influencing the management of cisplatin resistance observed in ovarian carcinoma [42]. These findings propose the potential utility of hsa-miR-1270 as a therapeutic target in addressing similar challenges within lung carcinoma.

MiR-1291 performs regulatory functions across wide range of cancer types through its ability to modulate cancer cell proliferation and metastasis via the targeting of numerous genes. By selectively inhibiting FOXA2-AGR2, it suppresses tumorigenesis in pancreatic cancer. It inhibits tumor invasion and progression in esophageal squamous cell carcinoma (SCC) via mucin 1 and regulates cell apoptosis. Furthermore, it suppresses renal cell carcinoma tumor growth by specifically targeting glucose transporter 1 [43, 44]. Our findings revealed an association between the downregulation of hsa-miR-1291 and the suppression of *KCNQ1*, alongside the overexpression of *KCNQ5*. Notably, prior research has not established a connection between hsa-miR-1291 and potassium voltage-gated channel-related genes.

The potential role of KCNQ1 has been emphasized in various human cancers, including cancer of colorectum, liver, esophagus, and renal cell [45, 46]. Consistent with our results, diminished expression of *KCNQ1* was noted in adenolung carcinoma (LUAD) compared to normal lung tissue. Additionally, an immunologically dynamic profile characterized by immune cell infiltration and modulation of immunomodulatory factors is associated with heightened levels of *KCNQ1*, contributing to the impediment of DNA replication and cell cycle progression [47, 48]. Notably, LUAD patients exhibiting low *KCNQ1* levels displayed favorable responses to treatment, with lapatinib emerging as a promising therapeutic option. These findings underscore the diagnostic and prognostic relevance of *KCNQ1*, emphasizing the potential for a tailored precision medicine approach in the management of LUAD [48]. Notably, *KCNQ5* overexpression was detected in squamous cell esophageal carcinoma compared to adenocarcinoma [49]. Furthermore, The possible interaction between celecoxib and KCNQ5 poses a promising opportunity for the prevention and treatment of several types of malignancies, such as colon, breast,

prostate, and head and neck cancers [50]. Delving deeper into the specific interplay between hsa-miR-1291 and KCNQ5 within lung carcinoma may yield valuable insights into the prognostic implications associated with hsa-miR-1291 expression levels.

Another target of hsa-miR-1291, *XYLT2*, has been a subject of interest in cancer research due to its involvement in glycosaminoglycan biosynthesis, particularly in the context of the extracellular matrix [51]. Notably, *XYLT2* overexpression promotes breast cancer cells migration and proliferation [52]. Moreover, it has been documented the diagnostic and prognostic role of *XYLT2* in gastric cancers [53]. Overexpression of XYLT2 was associated with aggressive LUAD [51]. These findings hint at *XYLT2*'s potential involvement in tumor aggressiveness and metastatic behavior, highlighting its potential involvement in tumor lung carcinoma progression and metastasis.

BCAN, member of the lectican family of chondroitin sulfate proteoglycans, has garnered attention in cancer research due to its involvement in tumor progression and its potential significance in cancer prognosis [54]. Lu, Wu (55) highlighted BCAN's role in glioma prognosis, associating its overexpression with poorer survival outcomes. Increased Brevican expression was also linked to adverse prognosis in breast cancer patients, particularly in promoting metastasis and tumor invasiveness [56]. In agreement with our findings, studies have demonstrated that hsa-miR-1291 can downregulate *BCAN* expression by directly binding to its mRNA, thereby affecting processes related to tumor progression and metastasis in different cancer types. This interaction between miR-1291 and *BCAN* highlights the regulatory role of miRNAs in modulating the tumor microenvironment and influencing cancer cell behavior.

Consistent with our results, previous research has shown that hsa-miR-1291 inhibits *BCAN* expression via direct binding to its mRNA, thus influencing tumor progression and metastasis processes in various types of cancer [57]. The correlation between miR-1291 and *BCAN* underscores the regulatory function that miRNAs perform by modulating the tumor microenvironment and impacting the behavior of cancer cells. These insights suggest a potential role for miR-1291 downregulation in the progression of LUSC.

Herein, we demonstrated that hsa-miR-485 was linked to the targeting of *KCNQ5, EDNRA, GNA14, GPC1,* and *VCAN*. Consistent with our findings, miR-485 exhibits downregulation in diverse cancer types, exerting significant roles in their progression and pathogenesis. Significantly, Wnt3a induces tumor suppressive effects in Retinoblastoma cells, which are partially ascribed to miR-485. Thus, miR-485 presents itself as a potentially effective therapeutic pathway for the management of Retinoblastoma [58]. Furthermore, emphasis has been placed on miR-485-5p's tumor suppressive function, demonstrated by its inhibition of growth and metastasis in small cell (SC)LC via targeting FLOT2 [59]

Elevated expression of *GPC1* has been identified in LUSC, serving as a discriminatory marker to effectively differentiate LUSC from LUAD with notable sensitivity

and specificity [60]. Furthermore, The high levels of exosomal GPC1 associated with the downregulation of miR-96-5p and miR-149 have been proposed as potential diagnostic biomarkers and adverse prognostic marker in CRC, according to prior research.[61, 62]. Substantial evidence from earlier studies has elucidated GPC1's role in tumor growth and angiogenesis [63, 64], emphasizing its function in promoting FGF-FGFR activation and downstream signaling pathways. [65].

Consequently, the identification of *GPC1* and *GPC5* among the crucial genes in our study suggests their potential roles in regulating cell signaling, proliferation, and differentiation within the context of LUSC. Their involvement in modulating tumor growth or cellular behaviors might indeed contribute to the observed pathogenesis, offering valuable insights into potential mechanisms underlying LUSC development.

Studies have highlighted the involvement of miR-485 in modulating cancer progression by targeting *EDNRA* and *GNA14*. Huang, Wu (66) demonstrated that miR-485 directly suppresses *EDNRA* expression, thereby impeding the progression of esophageal squamous cell. In colon cancer, *EDNRA* was associated with advanced tumor grade and stage [67, 68].Moreover, it has been that *GNA14* has tumor promoting role in colon [69] and epithelial cell cancer [70]. Interesting, Oshima, Ishikawa (71) demonstrated that miR-485 inhibits *GNA14* expression, attenuating the proliferation and metastasis of gastric cancer cells.

Another target linked to hsa-miR-485 was *VCAN*. Previous studies reported the potential role of VCAN as diagnostic maker in hepatocellular carcinoma (HCC) [72] and prognostic indicator in colon carcinoma [73]. Previous studies have delineated distinct mechanisms by which the proteoglycan, VCAN, influences tumor growth. Its G1 domain destabilizes cell adhesion, promoting proliferation, while the G3 domain activates the EGFR via EGF-like motifs, contributing to proliferation. Additionally, BCAN promote cancer invasion via EGFR signaling [74]. This collective evidence, coupled with our observed upregulation of genes *VCAN*, *BCAN*, and *EGFR*, underscores their intricate interconnections in driving LUSC progression. Further understanding of their crosstalk and mutual influence may unveil promising avenues for targeted therapies in LC management.

Intriguingly, *SDC4, VCAN, BCAN, XYLT2, GPC1* and *GPC5* been identified as genes associated with proteoglycan biogenesis [75]. The variability observed in genes responsible for proteoglycan biosynthesis holds significant relevance in the realm of cancer biology. These molecules wield influential roles within the tumor microenvironment, steering cellular signaling, proliferation, angiogenesis, modified cell adhesion, migration, and interactions with the extracellular matrix. Variations in the expression or functionality of these genes possess the capability to influence the extracellular matrix, thereby affecting the behaviors of tumors such as invasion, metastasis, and growth [76, 77].

Understanding the diversity of proteoglycan biosynthetic genes provides valuable information regarding the complex processes that regulate the progression and initiation of cancer. Acquiring this knowledge may open an avenue for novel therapeutic strategies that target these molecules, thereby facilitating control over the tumor microenvironment and possibly hindering the advancement of cancer. It is worth mentioning that proteoglycans possess the ability to regulate the activation and accessibility of a multitude of factors, including cytokines, growth factors, and hormones [78-80]. Tumor types of phenotypic diversity, gene expression, and recurrence rates are influenced by their function in these processes. Consequently, investigating variations of proteoglycan biosynthetic gene expression, its interactions, and its impact on tumor progression in lung carcinoma cells or tissues could unveil its potential significance and shed light on its involvement in lung cancer pathogenesis.

Our investigation revealed hsa-miR-19b-2 targeting *EDNRB, EDN1, GNAQ, KCND2, KCNH5, CACNA1C, EGFR,* and *KCNB2*. The upregulation of miR-19b-2 has been linked to tumorigenesis across diverse cancers, including lung cancer [81], nasopharyngeal carcinoma [82], and breast cancer [83], among others. Additionally, miR-19b-2 overexpression is implicated in promoting tumor migration and invasion in lung carcinoma. Notably, elevated miR-19b levels have shown promise as a prognostic biomarker in breast cancer and potentially impact tumor progression through the PI3K/AKT pathway [84].

Intriguingly, our findings of miR-19b-2-mediated *EDNRB* downregulation in LUSC align with previous observations linking reduced *EDNRB* expression to poor survival outcomes in LUAD [85] and observed suppression in HCC [86]. Furthermore, the prognostic significance of *EGFR* in LC has been previously reported [87, 88]. The binding of EDN1 to its receptor EDNRA has been associated with adverse outcomes in NSCLC, while EDN1-induced vasoconstriction limiting drug penetration into lung tumors could potentially compromise the effectiveness of EGFR TKI therapy, contributing to relapse [89]. These findings support the plausible role of these genes in LUSC progression.

On another note, *GNAQ* downregulation has been linked to metastasis in LC through the inhibition of extracellular-signal-regulated kinase (ERK) phosphorylation [90]. Additionally, Lu, Li (91) has highlighted *KCND2* overexpression's association with aggressive cancer behavior, emphasizing its prognostic relevance in LUAD. Similarly, KCNB2 has been associated with immunofiltration suppression, contributing to poor prognosis in LUAD. Similarly, Lyu, Wang (92) demonstrated the association of *KCNB2* with suppression of immunofiltration suppression, contributing to poor prognosis in LUAD. Though ion-channel gene hypomethylation was less frequent than hypermethyation, *KCNH5* hypomethylation and consequent overexpression was detected in NSCLC and served as predictor of poor prognosis in this cancer type [93]. Moreover, *CACNA1C* suppression has been correlated with unfavorable prognosis in LUAD [94]. Our findings emphasize the prognostic potential of miR-19b-2 due to its regulatory influence on these pivotal genes.

The current study demonstrated hsa-miR-4791 targeting *KCNQ5*. The observed reduction in hsa-miR-4791 expression has been identified in NSCLC [95], suggesting its potential as a biomarker for treatment in this specific cancer. Additionally, hsa-miR-4791 has been identified as a contributor to resistance against anti-EGFR treatment, thereby promoting tumor progression in NSCLC [96]. Our data underscores the role of calcium and potassium gated voltage channels in mediating progression and outcome of LUSC.

Our study revealed the upregulation of hsa-miR-2277 in LUSC, promoting *ERBB4* expression. Earlier research demonstrated marked upregulation of hsa-miR-2277 in multi-drug resistant SCLC [97]. MiR-2277 overexpression has been observed in prostate cancer animal model on high-fat diet, suggesting its involvement in cancer and metabolic pathways [98]. Furthermore, a study by illustrated that miR-2277-3p was overexpressed in colon cancer cells via liposome transfection and promoted cancer by targeting the cancer promoting gene, novel Nupr1-like isoform (*NUPR1L*). Herein, we demonstrated that miR-2277 promotes upregulation one of the critical genes, *ERBB4*. ERBB4 overexpression has been observed in NSCLC and has been linked to tumor aggressive behavior and poor prognosis [99, 100]. Moreover, loss of function mutation of *ERBB4* has been related to poor prognosis in advanced NSCLC.

Interestingly, our discovery that protein binding is associated with all 19 crucial genes, as revealed by the enrichment analysis, holds substantial significance. This correlation suggests that these genes may play a role in mediating fundamental cellular processes; thus, the significance of PPIs and their influence on cellular functions is highlighted. The enrichment analysis highlights the biological significance of these genes by providing insights into their participation in complex molecular processes. This may have implications for comprehending the pathogenesis of diseases, specifically in relation to the associations identified with LUSC in the present investigation.

To date, our investigation stands as the inaugural effort to integrate various bioinformatic methodologies. These include differential gene and miRNA expression analysis, the development of a prognostic model, prediction of target genes, and the visualization of PPIs networks. Our aim was to ascertain the importance of pivotal target genes associated with independently prognostic differentially expressed miRNAs in LUSC.

In summary, our research employed computational methodologies to develop a prognostic model for patients diagnosed with LUSC. This model incorporated the following 6 prognostic miRNAs: hsa-mir-1270, hsa-mir-19b-2, hsa-mir-2277, hsa-mir-4791, and hsa-mir-485-5p. The PPIs network uncovered 19 potentially critical target genes that were linked to these independent prognostic biomarkers, as determined by our analysis. It is worth mentioning that specific genes, namely *BCAN, VCAN, GNA14, SDC4,* and *KCNQ5,* did not possess pre-existing associations with LC. Conversely, *GPC1, EGFR, ERBB4, EDN1, EDNRA, EDNRB, KCNB2, KCND2, CACNA1C, XYLT2, KCNH5, GPC5, GNAQ,* and *KCNQ1* all possessed prior associations derived from previous

experiments or calculations. Based on these findings, prognostic miRNAs and their target genes may have significant utility in the future for targeted therapy and prognosis of LUSC, thereby providing novel diagnostic and therapeutic guidelines. Further clinical research is recommended to validate this prognostic model in LUSC patients and to investigate novel therapeutic approaches for those with unfavorable outcomes.

References

1. Sung H, Ferlay J, Siegel RL, Laversanne M, Soerjomataram I, Jemal A, et al. Global cancer statistics 2020: GLOBOCAN estimates of incidence and mortality worldwide for 36 cancers in 185 countries. CA: a cancer journal for clinicians. 2021;71(3):209-49.
2. John T, Cooper WA, Wright G, Siva S, Solomon B, Marshall HM, et al. Lung cancer in Australia. Journal of Thoracic Oncology. 2020;15(12):1809-14.
3. Howlader N. Seer cancer statistics review, 1975-2008, national cancer institute, bethesda, md. http://seer cancer gov/csr/1975_2008/, based on November 2010 SEER data submission, posted to the SEER web site. 2011.
4. AIHW. Cancer data in Australia. Australian Institute of Health and Welfare. 2020.
5. Thomas A, Liu SV, Subramaniam DS, Giaccone G. Refining the treatment of NSCLC according to histological and molecular subtypes. Nature reviews Clinical oncology. 2015;12(9):511-26.
6. Parker AL, Bowman E, Zingone A, Ryan BM, Cooper WA, Kohonen-Corish M, et al. Extracellular matrix profiles determine risk and prognosis of the squamous cell carcinoma subtype of non-small cell lung carcinoma. Genome Medicine. 2022;14(1):126.
7. Alwani A, Andreasik A, Szatanek R, Siedlar M, Baj-Krzyworzeka M. The role of miRNA in regulating the fate of monocytes in health and cancer. Biomolecules. 2022;12(1):100.
8. Diener C, Keller A, Meese E. Emerging concepts of miRNA therapeutics: from cells to clinic. Trends in Genetics. 2022;38(6):613-26.
9. Meng X, Eslami Y, Derafsh E, Saihood A, Emtiazi N, Yasamineh S, et al. The roles of different microRNAs in the regulation of cholesterol in viral hepatitis. Cell Communication and Signaling. 2023;21(1):231.
10. Ortiz GGR, Mohammadi Y, Nazari A, Ataeinaeini M, Kazemi P, Yasamineh S, et al. A state-of-the-art review on the MicroRNAs roles in hematopoietic stem cell aging and longevity. Cell Communication and Signaling. 2023;21(1):1-16.
11. Sargazi S, Mukhtar M, Rahdar A, Bilal M, Barani M, Díez-Pascual AM, et al. Opportunities and challenges of using high-sensitivity nanobiosensors to detect long noncoding RNAs: A preliminary review. International Journal of Biological Macromolecules. 2022;205:304-15.
12. Hu J, Stojanović J, Yasamineh S, Yasamineh P, Karuppannan SK, Hussain Dowlath MJ, et al. The potential use of microRNAs as a therapeutic strategy for SARS-CoV-2 infection. Archives of Virology. 2021;166:2649-72.
13. Gholizadeh O, Jafari MM, Zoobinparan R, Yasamineh S, Tabatabaie R, Akbarzadeh S, et al. Recent advances in treatment Crimean–Congo hemorrhagic fever virus: a concise overview. Microbial Pathogenesis. 2022;169:105657.
14. Yasamineh S, Yasamineh P, Kalajahi HG, Gholizadeh O, Yekanipour Z, Afkhami H, et al. A state-of-

the-art review on the recent advances of niosomes as a targeted drug delivery system. International journal of pharmaceutics. 2022;624:121878.

15.   Sadeghi MS, lotfi M, Soltani N, Farmani E, Fernandez JHO, Akhlaghitehrani S, et al. Recent advances on high-efficiency of microRNAs in different types of lung cancer: a comprehensive review. Cancer Cell International. 2023;23(1):284.

16.   Liang X, Wu Q, Wang Y, Li S. MicroRNAs as early diagnostic biomarkers for non-small cell lung cancer. Oncology Reports. 2023;49(1):1-12.

17.   Postow MA, Harding J, Wolchok JD. Targeting immune checkpoints: releasing the restraints on anti-tumor immunity for patients with melanoma. Cancer journal (Sudbury, Mass). 2012;18(2):153.

18.   Zhang L, Huang J, Yang N, Greshock J, Megraw MS, Giannakakis A, et al. microRNAs exhibit high frequency genomic alterations in human cancer. Proceedings of the National Academy of Sciences. 2006;103(24):9136-41.

19.   Yu S-L, Chen H-Y, Chang G-C, Chen C-Y, Chen H-W, Singh S, et al. MicroRNA signature predicts survival and relapse in lung cancer. Cancer cell. 2008;13(1):48-57.

20.   Wani JA, Majid S, Imtiyaz Z, Rehman MU, Alsaffar RM, Shah NN, et al. MiRNAs in Lung Cancer: Diagnostic, Prognostic, and Therapeutic Potential. Diagnostics (Basel). 2022;12(7).

21.   Wei L, Jin Z, Yang S, Xu Y, Zhu Y, Ji Y. TCGA-assembler 2: software pipeline for retrieval and processing of TCGA/CPTAC data. Bioinformatics. 2018;34(9):1615-7.

22.   Mohanad M, Yousef HF, Bahnassy AA. Epigenetic inactivation of DNA repair genes as promising prognostic and predictive biomarkers in urothelial bladder carcinoma patients. Molecular Genetics and Genomics. 2022;297(6):1671-87.

23.   Chen Y, Wang X. miRDB: an online database for prediction of functional microRNA targets. Nucleic Acids Research. 2019;48(D1):D127-D31.

24.   Szklarczyk D, Gable AL, Nastou KC, Lyon D, Kirsch R, Pyysalo S, et al. The STRING database in 2021: customizable protein–protein networks, and functional characterization of user-uploaded gene/measurement sets. Nucleic Acids Research. 2020;49(D1):D605-D12.

25.   Doncheva NT, Morris JH, Gorodkin J, Jensen LJ. Cytoscape StringApp: network analysis and visualization of proteomics data. Journal of proteome research. 2018;18(2):623-32.

26.   Scardoni G, Tosadori G, Faizan M, Spoto F, Fabbri F, Laudanna C. Biological network analysis with CentiScaPe: centralities and experimental dataset integration. F1000Res. 2014;3:139.

27.   Bader GD, Hogue CW. An automated method for finding molecular complexes in large protein interaction networks. BMC bioinformatics. 2003;4(1):1-27.

28.   Schwikowski B. The Cytoscape platform for network analysis and visualization. Chapman and Hall/CRC Press; 2019.

29.   Lee YS, Dutta A. MicroRNAs in cancer. Annual Review of Pathology: Mechanisms of Disease. 2009;4:199-227.

30.   Yi T, Zhou X, Sang K, Zhou J, Ge L. MicroRNA-1270 modulates papillary thyroid cancer cell development by regulating SCAI. Biomedicine & Pharmacotherapy. 2019;109:2357-64.

31.   Hu S, Song Y, Zhou Y, Jiao Y, Wang S. MiR-1270 Suppresses the Malignant Progression of Breast Cancer via Targeting MMD2. J Healthc Eng. 2022;2022:3677720.

32.   Wei L, Li P, Zhao C, Wang N, Wei N. Upregulation of microRNA-1270 suppressed human glioblastoma cancer cell proliferation migration and tumorigenesis by acting through WT1. Onco Targets Ther. 2019;12:4839-48.

33.   Zhong L, Zheng C, Fang H, Xu M, Chen B, Li C. MicroRNA-1270 is associated with poor prognosis and its inhibition yielded anticancer mechanisms in human osteosarcoma. IUBMB Life. 2018;70(7):625-32.

34.   Song Z, Wang J. LncRNA ASMTL-AS1/microRNA-1270 differentiate prognostic groups in gastric cancer and influence cell proliferation, migration and invasion. Bioengineered. 2022;13(1):1507-17.

35.   Ma R, Wang C, Wang J, Wang D, Xu J. miRNA–mRNA interaction network in non-small cell lung cancer. Interdisciplinary Sciences: Computational Life Sciences. 2016;8:209-19.

36.   Zhao Z, Han C, Liu J, Wang C, Wang Y, Cheng L. GPC5, a tumor suppressor, is regulated by miR-620 in lung adenocarcinoma. Molecular medicine reports. 2014;9(6):2540-6.

37.   Yang X, Chen Y, Zhou Y, Wu C, Li Q, Wu J, et al. GPC5 suppresses lung cancer progression and metastasis via intracellular CTDSP1/AhR/ARNT signaling axis and extracellular exosome secretion. Oncogene. 2021;40(25):4307-23.

38.   Li Y, Yang P. GPC5 gene and its related pathways in lung cancer. Journal of thoracic oncology. 2011;6(1):2-5.

39.   Gopal S, Arokiasamy S, Pataki C, Whiteford JR, Couchman JR. Syndecan receptors: pericellular regulators in development and inflammatory disease. Open biology. 2021;11(2):200377.

40.   Beauvais DM, Rapraeger AC. Syndecan-1-mediated cell spreading requires signaling by $\alpha v\beta 3$ integrins in human breast carcinoma cells. Experimental cell research. 2003;286(2):219-32.

41.   Mundhenke C, Meyer K, Drew S, Friedl A. Heparan sulfate proteoglycans as regulators of fibroblast growth factor-2 receptor binding in breast carcinomas. The American journal of pathology. 2002;160(1):185-94.

42.   Zhao Z, Ji M, Wang Q, He N, Li Y. Circular RNA Cdr1as upregulates SCAI to suppress cisplatin resistance in ovarian cancer via miR-1270 suppression. Molecular Therapy-Nucleic Acids. 2019;18:24-33.

43.   Luo H, Guo W, Wang F, You Y, Wang J, Chen X, et al. miR-1291 targets mucin 1 inhibiting cell proliferation and invasion to promote cell apoptosis in esophageal squamous cell carcinoma. Oncology Reports. 2015;34(5):2665-73.

44.   Yamasaki T, Seki N, Yoshino H, Itesako T, Yamada Y, Tatarano S, et al. Tumor-suppressive micro RNA-1291 directly regulates glucose transporter 1 in renal cell carcinoma. Cancer science. 2013;104(11):1411-9.

45.   Huang C, Li J, Zhang X, Xiong T, Ye J, Yu J, et al. The miR-140-5p/KLF9/KCNQ1 axis promotes the progression of renal cell carcinoma. The FASEB Journal. 2020;34(8):10623-39.

46.   Anderson KJ, Cormier RT, Scott PM. Role of ion channels in gastrointestinal cancer. World Journal of Gastroenterology. 2019;25(38):5732.

47.   Wang Y, Eldstrom J, Fedida D. Gating and regulation of KCNQ1 and KCNQ1+ KCNE1 channel complexes. Frontiers in Physiology. 2020;11:504.

48.   Chang KT, Wu HJ, Liu CW, Li CY, Lin HY. A Novel Role of Arrhythmia-Related Gene KCNQ1 Revealed by Multi-Omic Analysis: Theragnostic Value and Potential Mechanisms in Lung Adenocarcinoma. Int J Mol Sci. 2022;23(4).

49.   Polewko-Klim A, Zhu S, Wu W, Xie Y, Cai N, Zhang K, et al. Identification of Candidate Therapeutic Genes for More Precise Treatment of Esophageal Squamous Cell Carcinoma and Adenocarcinoma. Front Genet. 2022;13:844542.

50.   Tołoczko-Iwaniuk N, Dziemiańczyk-Pakieła D, Nowaszewska BK, Celińska-Janowicz K, Miltyk W. Celecoxib in cancer therapy and prevention–review. Current Drug Targets. 2019;20(3):302-15.

51.   Song Y-B, Bao W-G, Liu D-H, Wei L-Q, Yang S-T, Miao X-J, et al. Pan-cancer analysis of the prognostic significance and oncogenic role of GXYLT2. Medicine. 2023;102(46):e35664.

52.   Cui Q, Xing J, Gu Y, Nan X, Ma W, Chen Y, et al. GXYLT2 accelerates cell growth and migration by regulating the Notch pathway in human cancer cells. Experimental Cell Research. 2019;376(1):1-10.

53.   Zhao Y, Hu S, Zhang J, Cai Z, Wang S, Liu M, et al. Glucoside xylosyltransferase 2 as a diagnostic and prognostic marker in gastric cancer via comprehensive analysis. Bioengineered. 2021;12(1):5641-54.

54.   Wei J, Hu M, Huang K, Lin S, Du H. Roles of Proteoglycans and Glycosaminoglycans in Cancer Development and Progression. International Journal of Molecular Sciences. 2020;21(17):5983.

55.   Lu R, Wu C, Guo L, Liu Y, Mo W, Wang H, et al. The role of brevican in glioma: promoting tumor cell motility in vitro and in vivo. BMC cancer. 2012;12(1):1-10.

56.   Theocharis AD, Skandalis SS, Neill T, Multhaupt HA, Hubo M, Frey H, et al. Insights into the key roles of proteoglycans in breast cancer biology and translational medicine. Biochim Biophys Acta. 2015;1855(2):276-300.

57.   Wang J, Yokoyama Y, Hirose H, Shimomura Y, Bonkobara S, Itakura H, et al. Functional assessment of miR-1291 in colon cancer cells. Int J Oncol. 2022;60(2).

58.   Lyu X, Wang L, Lu J, Zhang H, Wang L. [Retracted] microRNA-485 inhibits the malignant behaviors of retinoblastoma by directly targeting Wnt3a. oncology reports. 2022;48(2):1-.

59.   Gao F, Wu H, Wang R, Guo Y, Zhang Z, Wang T, et al. MicroRNA-485-5p suppresses the proliferation, migration and invasion of small cell lung cancer cells by targeting flotillin-2. Bioengineered. 2019;10(1):1-12.

60.   Kai Y, Amatya VJ, Kushitani K, Kambara T, Suzuki R, Fujii Y, et al. Glypican-1 is a novel immunohistochemical marker to differentiate poorly differentiated squamous cell carcinoma from solid predominant adenocarcinoma of the lung. Transl Lung Cancer Res. 2021;10(2):766-75.

61.   Lu F, Chen S, Shi W, Su X, Wu H, Liu M. GPC1 promotes the growth and migration of colorectal cancer cells through regulating the TGF-β1/SMAD2 signaling pathway. Plos one. 2022;17(6):e0269094.

62.   Li J, Chen Y, Guo X, Zhou L, Jia Z, Peng Z, et al. GPC1 exosome and its regulatory miRNAs are specific markers for the detection and target therapy of colorectal cancer. Journal of Cellular and Molecular Medicine. 2017;21(5):838-47.

63.   Su G, Meyer K, Nandini CD, Qiao D, Salamat S, Friedl A. Glypican-1 is frequently overexpressed in human gliomas and enhances FGF-2 signaling in glioma cells. The American journal of pathology. 2006;168(6):2014-26.

64.   Aikawa T, Whipple CA, Lopez ME, Gunn J, Young A, Lander AD, et al. Glypican-1 modulates the angiogenic and metastatic potential of human and mouse cancer cells. The Journal of clinical investigation. 2008;118(1):89-99.

65.   Zhang Z, Coomans C, David G. Membrane heparan sulfate proteoglycan-supported FGF2-FGFR1 signaling: evidence in support of the "cooperative end structures" model. Journal of Biological Chemistry. 2001;276(45):41921-9.

66.   Huang T, Wu Z, Zhu S. The roles and mechanisms of the lncRNA-miRNA axis in the progression of esophageal cancer: a narrative review. Journal of Thoracic Disease. 2022;14(11):4545.

67.   Mahdi MR, Georges RB, Ali DM, Bedeer RF, Eltahry HM, Gabr A-EHZ, et al. Modulation of the Endothelin System in Colorectal Cancer Liver Metastasis: Influence of Epigenetic Mechanisms? Frontiers in Pharmacology. 2020;11.

68.   Mahdi MR, Bedeer RF, Eltahry HM, Berger MR. Aspects of the endothelin system in colorectal cancer. Biomedical Reviews. 2014;25:1-13.

69.   Park R, Lee S, Chin H, Nguyen AT, Lee D. Tumor-Promoting Role of GNA14 in Colon Cancer Development. Cancers (Basel). 2023;15(18).

70.   Jansen P, Müller H, Lodde GC, Zaremba A, Möller I, Sucker A, et al. GNA14, GNA11, and GNAQ Mutations Are Frequent in Benign but Not Malignant Cutaneous Vascular Tumors. Frontiers in Genetics. 2021;12.

71.   Oshima H, Ishikawa T, Yoshida GJ, Naoi K, Maeda Y, Naka K, et al. TNF-α/TNFR1 signaling promotes gastric tumorigenesis through induction of Noxo1 and Gna14 in tumor cells. Oncogene. 2014;33(29):3820-9.

72.   Naboulsi W, Megger DA, Bracht T, Kohl M, Turewicz M, Eisenacher M, et al. Quantitative tissue proteomics analysis reveals versican as potential biomarker for early-stage hepatocellular carcinoma. Journal of proteome research. 2016;15(1):38-47.

73.   Christov KT, Moon RC, Lantvit DD, Boone CW, Steele VE, Lubet RA, et al. 9-cis-retinoic acid but not 4-(hydroxyphenyl) retinamide inhibits prostate intraepithelial neoplasia in Noble rats. Cancer research. 2002;62(18):5178-82.

74.   Hu B, Kong LL, Matthews RT, Viapiano MS. The proteoglycan brevican binds to fibronectin after proteolytic cleavage and promotes glioma cell motility. J Biol Chem. 2008;283(36):24848-59.

75.   Noborn F, Nilsson J, Larson G. Site-specific glycosylation of proteoglycans: A revisited frontier in proteoglycan research. Matrix Biology. 2022;111:289-306.

76.   Mytilinaiou M, Nikitovic D, Berdiaki A, Kostouras A, Papoutsidakis A, Tsatsakis AM, et al. Emerging roles of syndecan 2 in epithelial and mesenchymal cancer progression. IUBMB life. 2017;69(11):824-33.

77.   Korpetinou A, Papachristou DJ, Lampropoulou A, Bouris P, Labropoulou VT, Noulas A, et al. Increased expression of serglycin in specific carcinomas and aggressive cancer cell lines. BioMed research international. 2015;2015.

78.   Nikitovic D, Mytilinaiou M, Berdiaki A, Karamanos N, Tzanakakis G. Heparan sulfate proteoglycans and heparin regulate melanoma cell functions. Biochimica et Biophysica Acta (BBA)-General Subjects. 2014;1840(8):2471-81.

79.   Voudouri K, Berdiaki A, Tzardi M, Tzanakakis GN, Nikitovic D. Insulin-like growth factor and epidermal growth factor signaling in breast cancer cell growth: focus on endocrine resistant disease. Analytical cellular pathology. 2015;2015.

80.   Farabaugh SM, Boone DN, Lee AV. Role of IGF1R in breast cancer subtypes, stemness, and lineage differentiation. Frontiers in endocrinology. 2015;6:59.

81.   Li J, Yang S, Yan W, Yang J, Qin YJ, Lin XL, et al. MicroRNA-19 triggers epithelial-mesenchymal transition of lung cancer cells accompanied by growth inhibition. Lab Invest. 2015;95(9):1056-70.

82.   Huang T, Yin L, Wu J, Gu JJ, Wu JZ, Chen D, et al. MicroRNA-19b-3p regulates nasopharyngeal carcinoma radiosensitivity by targeting TNFAIP3/NF-κB axis. J Exp Clin Cancer Res. 2016;35(1):188.

83.   Liu M, Yang R, Urrehman U, Ye C, Yan X, Cui S, et al. MiR-19b suppresses PTPRG to promote breast tumorigenesis. Oncotarget. 2016;7(39):64100-8.

84.   Li C, Zhang J, Ma Z, Zhang F, Yu W. miR-19b serves as a prognostic biomarker of breast cancer and promotes tumor progression through PI3K/AKT signaling pathway. OncoTargets and therapy. 2018:4087-95.

85.   Wei F, Ge Y, Li W, Wang X, Chen B. Role of endothelin receptor type B (EDNRB) in lung adenocarcinoma. Thorac Cancer. 2020;11(7):1885-90.

86.   Zhang L, Luo B, Dang Y-w, He R-q, Chen G, Peng Z-g, et al. The clinical significance of endothelin receptor type B in hepatocellular carcinoma and its potential molecular mechanism. Experimental and Molecular Pathology. 2019;107:141-57.

87.   Hendriks LE, Smit EF, Vosse BA, Mellema WW, Heideman DA, Bootsma GP, et al. EGFR mutated non-small cell lung cancer patients: more prone to development of bone and brain metastases? Lung cancer. 2014;84(1):86-91.

88.   Bahnassy AA, Ismail H, Mohanad M, El-Bastawisy A, Yousef HF. The prognostic role of PD-1, PD-L1, ALK, and ROS1 proteins expression in non-small cell lung carcinoma patients from Egypt. Journal of the Egyptian National Cancer Institute. 2022;34(1):23.

89.   Pulido I, Ollosi S, Aparisi S, Becker JH, Aliena-Valero A, Benet M, et al. Endothelin-1–Mediated Drug Resistance in EGFR-Mutant Non-Small Cell Lung Carcinoma. Cancer Research. 2020;80(19):4224-32.

90.   Choi JY, Lee YS, Shim DM, Lee YK, Seo SW. GNAQ knockdown promotes bone metastasis through epithelial-mesenchymal transition in lung cancer cells. Bone Joint Res. 2021;10(5):310-20.

91.   Lu X, Li K, Yang J. Potassium voltage-gated channel subfamily D member 2 induces an aggressive phenotype in lung adenocarcinoma. Neoplasma. 2021;68(1):135-43.

92.   Lyu Y, Wang Q, Liang J, Zhang L, Zhang H. The Ion Channel Gene KCNAB2 Is Associated with Poor Prognosis and Loss of Immune Infiltration in Lung Adenocarcinoma. Cells. 2022;11(21):3438.

93.   Ouadid-Ahidouch H, Rodat-Despoix L, Matifat F, Morin G, Ahidouch A. DNA methylation of channel-related genes in cancers. Biochimica et Biophysica Acta (BBA) - Biomembranes. 2015;1848(10, Part B):2621-8.

94.   Dasgupta S, Acharya S, Khan MA, Pramanik P, Marbut SM, Yunus F, et al. Frequent loss of CACNA1C, a calcium voltage-gated channel subunit is associated with lung adenocarcinoma progression and poor prognosis. Cancer Research. 2023;83(7_Supplement):3318-.

95.   Ma Y, Pan X, Xu P, Mi Y, Wang W, Wu X, et al. Plasma microRNA alterations between EGFR-activating mutational NSCLC patients with and without primary resistance to TKI. Oncotarget. 2017;8(51):88529-36.

96.   Pal AS, Bains M, Agredo A, Kasinski AL. Identification of microRNAs that promote erlotinib resistance in non-small cell lung cancer. Biochem Pharmacol. 2021;189:114154.

97.   Ma L, Li P, Wang R, Nan Y, Liu X, Jin F. Analysis of novel microRNA targets in drug-sensitive and -insensitive small cell lung cancer cell lines. Oncol Rep. 2016;35(3):1611-21.

98.   Duca RB, Massillo C, Dalton GN, Farré PL, Graña KD, Gardner K, et al. MiR-19b-3p and miR-101-3p as potential biomarkers for prostate cancer diagnosis and prognosis. American journal of cancer research. 2021;11(6):2802.

99.   Ma X, Li L, Tian T, Liu H, Li Q, Gao Q. Study of lung cancer regulatory network that involves erbB4 and tumor marker gene. Saudi Journal of Biological Sciences. 2017;24(3):649-57.

100.   Starr A, Greif J, Vexler A, Ashkenazy-Voghera M, Gladesh V, Rubin C, et al. ErbB4 increases the proliferation potential of human lung cancer cells and its blockage can be used as a target for anti-cancer therapy. International Journal of Cancer. 2006;119(2):269-74.